FABRICATION OF PHANTOM FOR QUALITY ASSURANCE ASSESSMENT IN CARDIAC SPECT IMAGING

by

MOHANNAD ADEL MUSTAFA SAYAH

Thesis submitted in fulfillment of the requirements
for the degree of
Doctor of Philosophy

April 2018

ACKNOWLEDGEMENT

All praises be to *Allah*, the beneficent and merciful one, who guides us in darkness and helps us in difficulties. I believe that Allah supports all efforts for a good cause. All praises be to *Muhammad*, the prophet (PBUH), who is the source of light in our minds.

I would like to thank the following groups/individuals who played a key role in this research: the School of Physics, Universiti Sains Malaysia in Penang for the opportunity to study and carry out my PhD research; Dr. Norlaili Ahmad Kabir, my main supervisor, who provided guidance, support, advice and assistance in my research; Professor Dr. Mohamad Suhaimi Jaafar, my co-supervisor, for his advice, expertise and helpful suggestions; academic staff and laboratory technicians for their cooperation and assistance; the Department of Nuclear Medicine at Institut Pergigian dan Perubatan Termaju (IPPT), Universiti Sains Malaysia, Penang, for the assistance in the completion of my experimental works; and Mr. Khairul Nizam Jaafar, IPPT, Universiti Sains Malaysia, Penang, for his assistance.

I extend my heartfelt gratitude and special regards to my family, especially to my father, who yearned for the day he would witness my success. I pray for him to be in *Allah*'s mercy. Although my father has left, he remains alive in my heart, and he will always be remembered. I would like to send all my regards and love to my mother for her prayers, assistance and care for my family in my absence. I would also like to extend my gratitude to Majeda, my elder sister, who is like a mother that sacrifices everything for others. I pray for you to be in *Allah's* peace. I am also grateful to Rima, my wife, for her endless encouragement, sacrifices and resilience amidst trials in my absence at our home in Jordan.

I would like to thank everyone who wishes for my success.

TABLE OF CONTENT

LIST OF TABLES

LIST OF FIGURES

Page

LIST OF ABBREVIATION

^{67}**Ga**	Gallium-67
^{99}**Mo**	Molybdenum-99
^{99m}**Tc**	Technetium-99m
^{111}**In**	Indium-111
^{123}**I**	Iodine-123
^{133}**Xe**	Xenon-133
^{201}**TI**	Thallium-201
A_W	Atomic weight
ANT	Anterior
C	Contrast
C_2H_4	Polyethylene
CA	Coronary Artery
CT	Computed Tomography
D	Distance
D	Mean pixels in centre of the defect
E	Energy
FWHM	Full Width Half Maximum
g/cm^3	Gram per cubic centimeter
IE	Intrinsic Efficiency
INF	Inferior
IPE	Intrinsic Peak Efficiency
keV	Kilo electron Volt
LAT	Lateral
LV	Left Ventricle
M	Mean pixels adjacent the defect
MBq	Mega Becquerel
MI	Myocardial Infarction
ml	Milliliter
MPI	Myocardial Perfusion Imaging
MPS	Myocardial Perfusion SPECT

MW	Myocardial Wall
MWLV	Myocardial Wall of Left Ventricle
N_e	Number of photons in full energy peak
N_A	Avogadro number
N_0	Number of electrons per gram
Pb	Lead
PET	Positron Emission Tomography
QC	Quality centre
R	Resolution
S	Number of the photons emitted by the source
SEP	Septal
SPECT	Single Photon Emission Computed Tomography
TE	Total Efficiency
Z	Atomic number
Z_{eff}	Effective atomic number
γ	Gamma
μ	Linear attenuation coefficient
μCi	Micro curie
Ω	Solid angle between the detector and the source
Φ	Acceptance angle
$B(f)$	Butterworth filter
a	Radius of the detector
f	Distance between the detector and the source
f	Spatial frequency domain
f_c	Critical frequency
n	Order of the filter

FABRIKASI FANTOM UNTUK PENAKSIRAN JAMINAN KUALITI DALAM PENGIMEJAN SPECT KARDIAK

ABSTRAK

Pemancaran Foton Tunggal Tomografi Berkomputer (SPECT) sering digunakan untuk pengimejan bagi pengenalpastian infarksi miokardium di dalam saluran dinding miokardial. SPECT mampu mengenalpasti kawasan-kawasan penginfarkan dalam MW. Dalam kajian ini, satu fantom penginfarkan miokardial telah difabrikasi dan direkacipta untuk mensimulasi MW pada ventrikel kiri (MWLV) pada peringkat hujung sistol dan hujung diastol. Kajian ini bertujuan menilai fantom MI pada kedua-dua peringkat sebagai sebahagian daripada penilaian jaminan kualiti dalam pengimejan SPECT kardiak. Di peringkat hujung diastol, apabila kecacatam berada pada dinding depan dan bawah, ketebalan minima yang dapat dikesan ialah 2 mm tanpa mengira kedudukan fantom pada meja pengimejan. Apabila kecacatan berada di kawasan tengah, kejelasan kecacatan dapat diperhatikan pada ketebalan minima 3 mm. Apabila kecacatan berada di kawasan puncak dan bawah, kejelasan kecacatan hanya dapat dilihat apabila kecacatan mempunyai ketebalan minima berukuran 4 mm. Pada peringkat hujung-sistol, ketebalan minima yang dikesan ialah 3 dan 2 mm apabila kecacatan diperhatikan pada kawasan depan dan bawah, tidak kira kedudukan fantom di atas meja pengimejan. Apabila fantom bergerak dari pusat tersebut sehingga 15 cm jauh dari pusat, kejelasan dapat diperhatikan pada kecacatan dengan ketebalan minima 4 mm, tidak kira kawasan, iaitu tengah, puncak dan bawah. Peratusan pembesaran kecacatan di da dalam imej SPECT ialah 94% sehingga 106% pada hujung diastol, dan bersamaan 98% sehingga 110% pada hujung sistol, apabila fantom dijauhkan dari posisi tengah meja pengimejan. Kedudukan

fantom MI di tengah-tengah dan kelebaran jendela tenaga (15%) amat penting untuk menghasilkan imej-imej SPECT dengan nilai kontras yang ketara dengan nilai 0.31. Jendela tenaga (20% dan 25%) dengan kedudukan eksentrik (jauh dari tengah) menghasilan imej-imej SPECT dengan nilai kontras yang rendah iaitu 0.25, terutama apabila kecacatannya terletak di kawasan bawah

FABRICATION OF PHANTOM FOR QUALITY ASSURANCE ASSESSMENT IN CARDIAC SPECT IMAGING

ABSTRACT

Single-photon emission computed tomography (SPECT) is commonly used in nuclear imaging to detect myocardial infarction (MI) within a myocardial wall (MW). SPECT can identify areas of infarction in MW. In this work, a MI phantom was fabricated and designed to simulate the MW of the left ventricle (MWLV) in the end-diastole and end-systole stages. This work aimed to assess the MI phantom in both stages as a part of quality assurance assessment in cardiac SPECT imaging. In the end-diastole stage, when the defects were fixed at the anterior and inferior walls, the minimum detectable thickness was 2 mm regardless of the position of the phantom on the imaging table. When the defects were placed in the mid-region, the clarity of the defects could be observed at a minimum thickness of 3 mm. When defects were placed in the apex and basal regions, the clarity of the defects was only visible when the defects possessed a minimum thickness of 4 mm. In the end-systole stage, the minimum detectable thicknesses were 3 and 2 mm when the defects were placed at the anterior and inferior regions, respectively, regardless of the phantom position on the imaging table. The minimum detectable thickness of defects fixed in the septal and lateral regions was affected by the position of the phantom on the imaging table. When the phantom was moved from the centre to 15 cm away from the centre, the clarities were observed only in defects with a minimum thickness of 4 mm regardless of the regions, that is, mid, apex or basal. The Magnification percentage of defect area is at 94% to 106% at end diastole stage, and is at 98% to 110% at end systole stage, when the MI phantom was

moved away from centre to off-centre of the imaging table. The positions of the MI phantom at the centre and energy window width (15%) were necessary to produce SPECT images with the highest contrast value at 0.31. Energy window (20% and 25%) with off-centre positioning produced SPECT images with low contrast value at 0.25, particularly when defects were located in the inferior region.

CHAPTER 1

INTRODUCTION

1.1 Background

Roentgen Wilhelm, with his impressive discovery of X-rays, founded the fundamentals of X-ray imaging. The discovery was entitled “On a New Kind of X-ray” and published in Physical Medical Society of Wurtzburg in December 1985 (Röntgen, 1895). The famous X-ray photograph was taken from the left hand of his wife (Figure 1.1). Since then, numerous X-ray applications have been utilised in the medical field.

Figure 1.1: First X-ray image (Röntgen, 1895)

Medical imaging technology has advanced from radiography to nuclear medicine to provide the physiological and biochemical information on acquired images. In the 1950s, researchers enhanced their understanding of the detection of the ionizing

radiation of radionuclides. (Anger, 1952) introduced a gamma camera as a novel detection tool to localise the distribution of an administered radionuclide. His original prototype in 1952 was a camera, in which a photographic X-ray film was in contact with a NaI(Tl)-intensifying screen (Anger, 1952).

Nuclear medicine imaging is based on the external detection of a biodistributed radiotracer administered to a patient. In this technique, small amounts of radioactive materials are typically injected into the bloodstream or orally administered (Brant & Helms, 2012). Several different radiotracers are used to study various parts of the body. A radiotracer travels through an area subjected to examination and releases energy in the form of ionizing radiation, which is detected by a special camera. Computational techniques are then applied to reconstruct images. In clinical practice, almost all nuclear medicine procedures that use single-photon-emission tracers rely on a gamma camera. A multihole collimator is mounted on the front face of a system to provide a spatial correlation of the detected events and localise the emission site of the released photons (Cherry et al., 2012).

SPECT has emerged as a routine procedure in most nuclear medicine departments since the concept was first introduced in the 1960s (Groch & Erwin, 2000). This technology has been further enhanced when modern medical imaging technologies have been improved. Current medical imaging techniques require the use of a computer for acquisition and image reconstruction. SPECT imaging provides sliced images in the transverse, sagittal or coronal planes; for cardiac applications, images are reoriented into oblique short and long-axis slices (Saha, 2012). SPECT is a tomographic reconstruction technique applied in nuclear medicine, and SPECT reconstruction allows the

localisation of radiation signals of internal organ structures for critical patient diagnosis and management (Cherry et al., 2012). SPECT is also a type of functional imaging technique that uses radionuclides to detect anatomical and physiological information.

A small dose of radionuclide is used to measure changes in cells/tissues (Müller & Schibli, 2013). Dose may be adjusted according to patient weight; for example, a heart tissue uptakes 2.5% of the total dose of ^{99m}Tc (Flotats & Carrió, 2006). The radionuclide absorption rate is relatively different between healthy and unhealthy tissues.

MI is defined as cell death due to myocardial ischaemia, that is, inadequate myocardial blood flow (Rajiah et al., 2013; Thygesen et al., 2012). Classical MI results from a plaque rupture in a coronary artery leading to an occluding blood clot at the site of the rupture, thereby possibly causing sudden death (Makkar et al., 2012). Initially, myocardial cell death occurs in the subendocardium, which is located in the inner layer of the left ventricular (LV) wall (Thygesen et al., 2012). Infarcts are usually classified according to their size (small, <10% of the LV); medium, 10% to 30% of the LV; or large, >30% of the LV) and location (anterior, inferior, septal, lateral or a combination of these locations) (Antman et al., 2000).

MI can be clinically categorize as transmural and nontransmural based on anatomical features (Bolooki & Askari, 2010). Abnormalities in myocardial wall (MW) thickness (MWT) occur early in ischaemia, and absence or weakness of MWT is closely related to decreased subendocardial blood flow (Duerinckx, 2001). A transmural MI is characterised by full thickness of the affected muscle segment(s), whereas a non-

transmural MI is defined as an area of infarction that does not extend through the full thickness of MW segments (Bolooki & Askari, 2010). The area of non-transmural MI is limited and is the least perfused region of the heart. The types of MI should be clinically identified to classify its severity.

Infarcts can be directly visualised by SPECT. In the detection of MI size through SPECT, radioactive tracers, namely, ^{201}TI and ^{99m}Tc-labelled agents, are used to assess MI (Sridhara et al., 1993). Reconstructed images reflect the radioactivity distribution of a tracer in the LV. The pixel intensities of the SPECT images are then measured. A pixel intensity of >50% of the maximum value represents normal perfusion (hot), and the myocardium is considered viable. If the pixel intensities are <50% (cold) of the maximum value, the myocardium is regarded as non-viable (Hansen et al., 2006; Oliveira et al., 2013).

Phantoms are used for many applications in the field of nuclear medicine imaging. Phantoms are utilised in two different purposes, namely, quality assurance (QA) and control and specific anatomical resemblance. A high-quality phantom should closely mimic imaging routines. A phantom that resembles a region of a human body is called an anthropomorphic phantom (Cannon et al., 2009). This phantom must be built with tissue-equivalent materials to represent true clinical attenuation conditions.

1.2 Problem Statement

Non-transmural infarcts or small defects may remain unnoticed with the use of SPECT, and patients with prior MI before death exhibit subendocardial infarcts (small defects) (Mahrholdt et al., 2003). Subendocardial infarcts are missed by SPECT because of the

low spatial resolution of SPECT (Ibrahim et al., 2007; Wagner et al., 2003). To date, there is no MI phantom to simulate the threshold value of non-transmural infarct thickness placed at different location within MI phantom that able to be detected by SPECT system.

Incorrect positioning may lead to formation of artifacts. Also, incorrect positioning with respect to the patient table that lead the formation of artefacts may decrease the quality of SPECT images. Other parameters, such as the energy window width also play an important role in the quality of SPECT images. Correct energy window width and patient positioning has always been the factors of recommendation to avoid image artefacts that can affect diagnostic accuracy. Most photons with energies less than 60 keV are attenuated in the patient's body, whereas photons with higher energies cause scattering. Therefore, the optimal energy width should be set in the best range.

Images with poor quality and pixel uniformity likely lead to false diagnosis. Energy widow width and positioning on an imaging table may affect on detection quality in myocardial SPECT imaging. This is a research project to study how the positioning and energy window width setting affect minimum detectable myocardium infarction thickness and its area. To support the research, a specific phantom will be fabricated to simulate the myocardium wall tissues and myocardium infarction tissues. This is mainly because, the myocardium wall thickness from diastole to systole stage may cause partial volume effects (PVE), which is one of the main factors affecting SPECT image quality.

1.3 Objective of Research

This study aims to design and fabricate a cardiac phantom with various transmural thicknesses for QA of myocardial SPECT imaging. The specific objectives are as followed:

i. To fabricate a MI phantom to mimic the effective atomic number, density, and thickness values of myocardium and myocardium infarction.
ii. To quantify the uniformity of pixel intensity distribution responding to the distribution of ^{99m}Tc within the MI phantom.
iii. To determine the minimum MI thickness able to be resolved by the SPECT imaging system.
iv. To measure the surface area of MI on SPECT images using ImageJ software.
v. To study the effect of energy window and position of the MI phantom on image contrast.

1.4 Scope of Research

This research introduced two fabricated MI phantoms of polyethylene plastic to simulate MWLV. The MI phantoms were designed to mimic MWLV in cases of end-diastole and end-systole stages. Rectangular defects of plastic were also constructed to simulate various thicknesses of MI in MWLV. These MI phantoms in end-diastole and end-systole stages with various MI thicknesses can be used in the QA of myocardial SPECT imaging in nuclear medicine. In this research, SPECT system and MI phantom at end-diastole and end-systole stage were investigated

1.5 Structure of Thesis

The work summarised in this thesis aimed to evaluate myocardial SPECT image in the presence of MI defects. The content of this thesis is organised as followed.

Chapter 1 briefly presents a general introduction on the role of SPECT imaging as an important part of medical imaging in the assessment and detection of infarction (defect) within MW. This chapter also lists the research problems, objectives and scope of this thesis.

Chapter 2 discusses the theoretical and medical basis of MI (defect) occurrence and provides an overview of the ability of SPECT to assess MI (defect) by using various methods and parameters, such as cardiac positioning and distance, defect location, energy window width and common SPECT filters, which can contribute to SPECT image formation. This chapter also presents an overview of the physical characteristics of ^{99m}Tc as a labelled isotope used in myocardial SPECT imaging.

Chapter 3 describes the materials and methods used in this study, including the preparation of ^{99m}Tc injected into the side phantom, the fabrication of phantom material and design, acquisition of SPECT images, and the positioning of the phantom on the imaging table.

Chapter 4 presents the results and discusses the uniformity in the reconstructed SPECT images at end-diastole and end-systole stages at different positions on an imaging table and the ratio of the mean pixel value of anterior/inferior and septal/lateral of myocardial SPECT images. This chapter further explains the minimum detectable

defect thickness, area of defect and contrast. The effects of energy window and phantom positions on contrast were explained.

Chapter 5 summarises the study, and provides recommendations for future studies.

CHAPTER 2

LITERATURE REVIEW

2.1 Background

SPECT has been routinely used to detect MI in myocardial perfusion imaging (MPI) (Jaszczak, 2006). It is used to measure and assess the MW at risk, infarct size and treatment efficiency of acute MI (Gibbons et al., 2000). SPECT is one of the techniques used to provide useful information on the physiologic function of an organ and detect the presence of lesions by image reconstruction. Several clinical studies on SPECT showed that measuring defect size within MW is very important for the accuracy of determining MI severity (Oliveira et al., 2013; Takagawa et al., 2007).

Detecting small MI (non-transmural) is difficult due to the limited resolution of SPECT. MPI using SPECT is considerably poor in the detection of subendocardial defects (Ibrahim et al., 2007). SPECT is limited in assigning perfusion defects to their corresponding coronary lesion, which is a main prerequisite for accurate therapy planning. MI misdiagnosis is the major cause of therapy delays (Dadkhah et al., 2007). The location and thickness of the defect within the MW are significant factors for detecting defects (Elkamhawy & Chandna, 2001).

SPECT infarct size is closely associated with real fibrosis in human hearts (Maes et al., 1997). The non-invasive assessment of infarct size is a useful clinical tool for risk stratification (Gibbons et al., 2004).

Myocardial perfusion SPECT (MPS) has been used as a reference method to estimate infarct size based on visual qualitative evaluation of perfusion defect (Gibbons et al., 2004). SPECT polar map method is used to determine infarct size (defect) for risk assessment. This method provides a calculation of the defect size as a percentage of the LV. The size of the defect is calculated by a threshold value of 50% of the maximum grey value (Cuberas-Borrós et al., 2013; Slomka et al., 2012). Perfusion defect size that is assessed via MPS is comparable with that obtained through a histological evaluation of infarct size in of the effects of ischaemic cardiomyopathy (Medrano et al., 1996).

Cardiac phantoms in nuclear medicine can be classified into static and dynamic phantoms. Static phantoms yield information on radioactive tracer location in myocardium. Therefore, they are generally used for cardiac perfusion measurements. Dynamic cardiac phantom simulates ventricle operation and is controlled with the assistance of a computer to detect movement of radioactive tracer in and out of the ventricle.

For perfect quality of SPECT images, detector must work in best conditions to avoid non-uniformity of isotope distribution within organs (Baron & Chouraqui, 1996). Transmission source can obtain the attenuation coefficients to correct non-uniformity of SPECT image. (Du Raan et al., 2000; O'Connor & Kemp, 2006).

2.2 Cardiovascular System

The heart is an organ that pumps blood throughout the body via the circulatory system to supply nutrients and oxygen to all tissues in the body. The heart consists of four main chambers, two at the right and two at the left that pumps blood throughout the body.

One of these chambers is the LV, as shown in Figure 2.1. The LV is the thickest wall of the heart chambers and is responsible for pumping oxygenated blood to all tissues in the body, and this task is dependent on the strength of myocardial wall (Movahed et al., 2009). The MWLV is a muscle similar to other muscles because it requires blood to feed its tissue. If blood flow is cut off at a section of MWLV, tissues at the section die, causing an infarction.

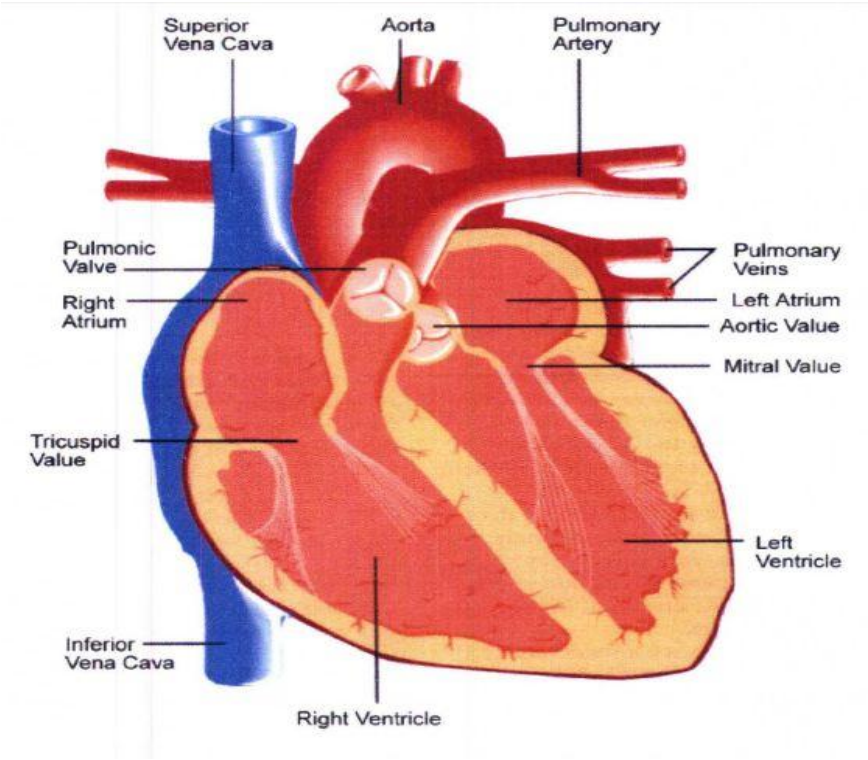

Figure 2.1: Cross section of the heart (Nguyen, 2010)

2.2.1 Myocardial Wall

Diastole and systole are parts of the cardiac stage that generates difference in blood pressure. Systolic pressure occurs when the LV contracts to push blood in the body, whereas diastolic pressure arises from the extension of the LV. During contraction and

extension, the heart exhibits different MWLV thickness, as shown in Figure 2.2. The difference in wall thickness affects the size of myocardial wall. Therefore, the thickness the difference in wall thickness is affected by diastolic and systolic.

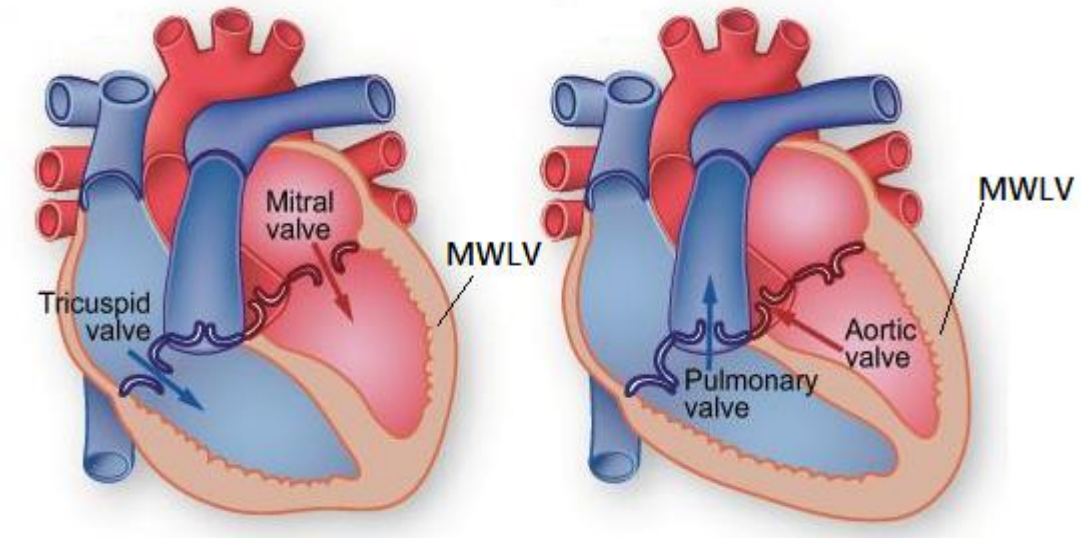

Figure 2.2: Heart in two configurations, namely, left side end diastole and right side end systole (Lorraine T. Nott & Dayville, 2016)

2.3 Myocardial Infarction (MI)

MI occurs due to the obstruction within the coronary artery system (Thygesen et al., 2012). The coronary vascular system is the major supplier of nutrition and oxygen for the body. MI is known as heart attack. It is a condition of partial tissue death within cardiac muscles. This occurs when one or more coronary arteries, which provide oxygen-rich blood to cardiac muscle, become suddenly closed. Blockage is caused by plaques, which consists of cholesterol, fats and other substances (Thygesen et al., 2012). When a coronary artery (CA) is obstructed, the downstream myocardium is restricted of oxygen and nutrition, resulting in myocardium ischaemia, as shown in Figure 2.3.

Furthermore, prolonged ischaemia causes enlarge the area of dead tissue within the MW.

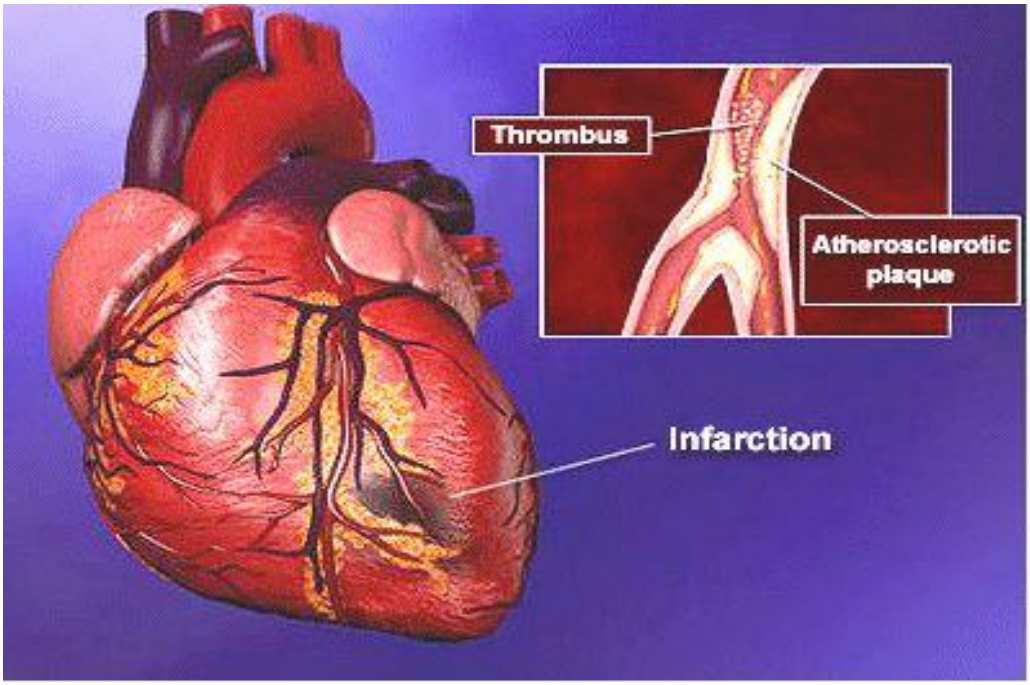

Figure 2.3: Obstruction of coronary artery with an infarction in myocardial wall of left ventricle (Lorraine T. Nott & Dayville, 2016)

2.4 Radiopharmaceutical Tracers

2.4.1 ^{99m}Tc

The ^{99m}Tc isotope has been first isolated in 1938 by Seaborg and Segrè (Seaborg & Segrè, 1939). ^{99m}Tc was not used as a medical tracer until 1960 (Herbert et al., 1965; Sorensen & Archambault, 1963). ^{99m}Tc is a pure γ-emitter of 140 keV photon energy with a half-life of 6 hours, and its half-life properties are presented in Table 2.1.

Table 2.1: Half-life properties of ^{99m}Tc (Movahed et al., 2009)

Physical half-life	6 hours
Biological half-life	24 hours
Effective half life	5 hours

^{99m}Tc is an isotope used in nuclear medicine for diagnostic imaging by studying the functional uptake of the ^{99m}Tc by the organ of interest. ^{99m}Tc is practically useful for nuclear medicine procedures because ^{99m}Tc can be chemically incorporated into small-molecule ligands and protein that concentrate in specific organs or tissue when injected into the body.

2.4.1(a) Physical Decay of ^{99m}Tc

^{99m}Tc decay occurs at a half-life of 6.02 hours. The physical decay of ^{99m}Tc is relative to its half-time, as shown in Table 2.2.

Table 2.2: Physical decay of ^{99m}Tc at 6.02 hours half-life (Healthcare, 2005)

Hours	% Disintegration
0	100
1	89
2	79
3	70
4	63
5	56
6	50

The relatively short physical half-life of ^{99m}Tc allows SPECT imaging procedures to collect data quickly. Moreover, ^{99m}Tc is the suitable isotope used in nuclear imaging, specifically in myocardial SPECT imaging, because of its distinctive characteristics fit for the biological properties of heart muscle tissue.

2.4.1(b) ^{99m}Tc Generator

The transition of γ-ray from ^{99m}Tc to decayed ^{99}Tc occurs at around 6 hours, as shown in Figure 2.4. ^{99m}Tc offers the advantage of allowing production in a table top generator from its parent ^{99}Mo. Thus, it is relatively cheap and easily available. When chemically reduced, it can unite with a wide range of compounds without changing their properties.

.

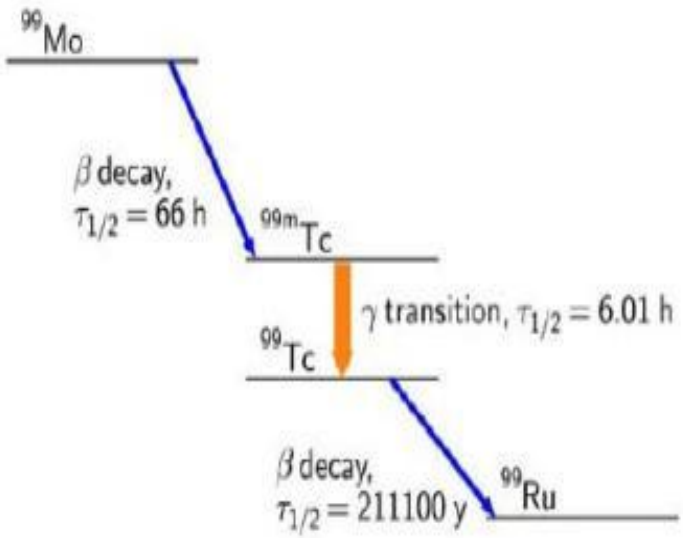

Figure 2.4: Demonstration of Tc-99m decay to Tc-99 with of 6 hours half life transition (Glover & Gropler, 2007)

2.5 Nuclear Medicine Imaging Basics

In diagnostic nuclear medicine, trace amounts of radioactivity is managed to provide information of diagnostic importance. A radionuclide that emits gamma photons is labelled with a target-specific pharmaceutical to produce a radiopharmaceutical, which is administered to the patient. Gamma rays are emitted with the decay of the administered radiopharmaceutical and then detected using an exterior gamma camera, as shown in Figure 2.5.

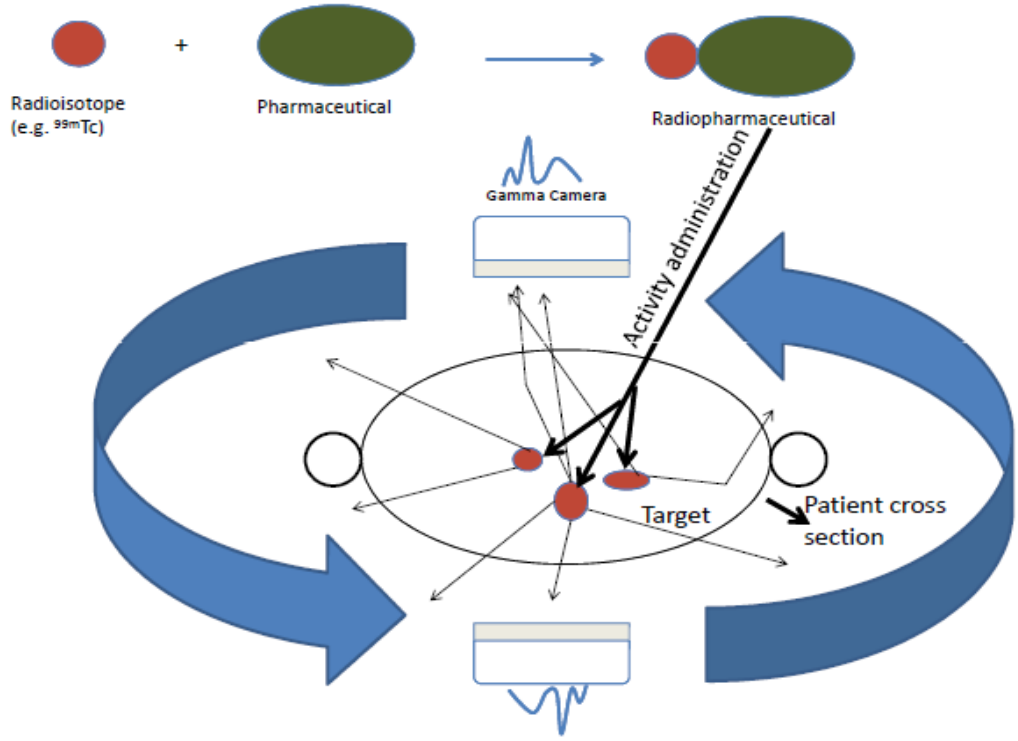

Figure 2.5: Schematic of SPECT from radiopharmaceutical synthesis to acquisition of SPECT projection data (Karamat, 2012)

2.5.1 Nuclear Medicine Image Acquisition

In the first stage of nuclear medicine imaging, a radiopharmaceutical substance is administered into a patient's body. In the next stage, emitted γ-photons are detected by using an external detection system. This external detector system is called a gamma camera, and its main components are a collimator, a scintillation crystal and a computer.

The following three physical phenomena are central to quantitative SPECT interference: photon attenuation, photon scatter and distance-dependent resolution (King et al., 2004). Attenuation is a physical factor effect on the diagnostic quality and quantitative accuracy of SPECT (Corbett et al., 2004). Photon attenuation strongly reduces the quantitative and diagnostic accuracy in cardiac SPECT imaging (Bateman & Cullom, 2005). The γ-rays measured by the detector are based on the rays' intensity value *I*. The μ is the linear attenuation coefficient of the object and is dependent on its composition, and S is the path length from the gamma source and the detector inside the camera head. These variables are expressed in equation as follows:

$$I = I_O e^{-\int \mu(x) ds} \tag{2.1}$$

$$I = I_O e^{-\Sigma \mu x} \tag{2.2}$$

$$\frac{I}{I_O} = e^{-\Sigma \mu x} \tag{2.3}$$

$\frac{I}{I_o}$ is the total transmission of γ-rays within the path between the γ-source on the imaging table and the detector inside the γ-camera head.

This transmission strongly depends on the path length between the γ-source and detector inside the camera; thus, γ-source positioning on an imaging table can alter the path length. Variation in the ability of γ-rays to reach the detector may result to variable SPECT image quality.

2.5.2 Collimator

To image the activity distribution accurately, the camera selectively takes in the gamma ray with the aid of a collimator. A collimator is the main part of a SPECT gamma camera because the former symmetrically adjusts between the position of the γ-photons within the target and the collimator's detected position on the detector crystal. A collimator allows γ-photons that are parallel to the hole orientation to pass through. Collimators are generally classified on the basis of their hole orientation and energy range.

The collimator acts as a lens for the imaging system by rejecting gamma rays with undesirable trajectories. In a parallel-hole collimator, the holes are arranged parallel to each other and perpendicular to the imaging plane. The configuration only allows the passage of γ-rays that are approximately perpendicular to the imaging plane. As such, this process is useful for image formation. The gamma rays that pass through the collimator impinge onto the scintillation crystal, which converts the rays into light. The amplified electrical signal is then passed through the circuits, which combine signals from adjacent photomultiplier tubes, to determine the position of the original gamma rays interacting with the scintillation crystal. These locations are transferred to a computer that tabulates successive gamma ray detection events into a 2D array, which is

a projection of the radioactive distribution. In SPECT, these projections are acquired at multiple angles around the patient.

2.5.3 Detection Efficiency

The gamma photons must initially undergo a significant interaction within the detector before the detection process can begin. The gamma photons may travel a long mean free path and remain undetected despite passing through the detector. Absolute efficiency and intrinsic detection efficiency are two kinds of efficiencies generally considered in gamma ray detection. The total efficiency of the detectors is defined as the fraction of the total number of gamma photons emitted from the gamma source that is recorded by the detector. Such parameter is expressed as:

$$TE = \frac{number\ of\ photons\ recorded}{number\ of\ the\ photons\ emitted} \tag{2.4}$$

The intrinsic efficiency is defined as

$$IE = \frac{number\ of\ photons\ recorded}{number\ of\ the\ photons\ incident\ on\ \ detector} \tag{2.5}$$

Where (TE) is the total efficiency and (IE) is the intrinsic efficiency.

The total efficiency includes the absolute efficiency, which depends on the geometry of the setup, whereas the intrinsic efficiency depends on the physical thickness of the detector in the orientation of the incident photons and the distance (*f*) between the emitted source and the detector.

The most common type of efficiency tabulated for gamma detectors is the intrinsic peak efficiency (IPE) given by (Knoll, 2000):

$$IPE = \frac{4\pi Ne}{S\Omega} \tag{2.6}$$

where

N_e is the number of photons in a full energy peak of the detector spectrum,

S is the number of the photons emitted by the source higher than the measurement period and

Ω is the solid angle between the detector and the source. Ω is defined as

$$\Omega = 2\pi\left(1 - \frac{f}{\sqrt{f^2+a^2}}\right) \tag{2.7}$$

where

f is the distance between the detector and the emitted source and

a is the radius of the detector.

Hence, the above-mentioned relations indicate that the detection efficiency is affected by the distance between the detector placed within the collimator and the source, which holds the radionuclide (e.g. ^{99m}Tc) within the organ or phantom.

2.5.4 Spatial Resolution

The loss of spatial resolution is a crucial cause of SPECT image quality degradation. This loss is due to the physical collimator on the γ-camera and the intrinsic spatial detection resolution and correlated with the positioning and distance of the γ-source on

an imaging table below the camera's head routes. The collimator consists of a series of holes separated by septa.

Actually, the image's spatial resolution is a function of the distance between the head camera, which includes the collimator, and the γ-ray source (Cherry et al., 2012). This relation is referred to as distance-dependent resolution. The following equation can be used to describe distance (D)-dependent resolution (Sabondjian, 2010):

$$R = D \cdot \tan(\Phi) \tag{2.8}$$

where

R is the resolution,

D is the distance between the γ-source and crystal inside the camera head collimator and

Φ is the acceptance angle.

2.5.5 Energy Resolution

The image quality is highly dependent on the selected energy width (Rong et al., 2012). In conventional SPECT scanning, the gamma emitter radioisotopes with a stated energy window of the photo peak, such as ^{99m}Tc (140 keV), are used for SPECT imaging (H. Zeng et al., 2014). To study the effect of the energy width on the image acquisition with different energies, scholars obtain the width setting by using the mode acquisition of a myocardial phantom with defect inserts. Various acquisitions in myocardial SPECT imaging undergo several acquisition stages and involve different parameters, such as the energy window, heart motion and respiration.

The full width at half maximum (FWHM) is shown in Figure 2.6 and defined as the distribution width at the half-maximum level of the photon peak (G. Knoll, 2000). The previous definition supposes that any continuum or background on which the photon peak may be superimposed is negligible or has been subtracted away. The energy resolution of the detector is the detector ability to reduce the narrow peak in the photon spectrum. Energy resolution is affected by many factors, such as detector geometry and electronic noise. The resolution (R) of a SPECT image is calculated through the percentage of a dimensionless fraction and thus conventionally expressed through the following relation (G. F. Knoll, 2010):

$$R = \frac{FWHM}{E} \qquad 2.9$$

Where

(R) is the percentage of the resolution,

(FWHM) is the full width at half maximum and

(E) is the energy at the centre of the photon peak.

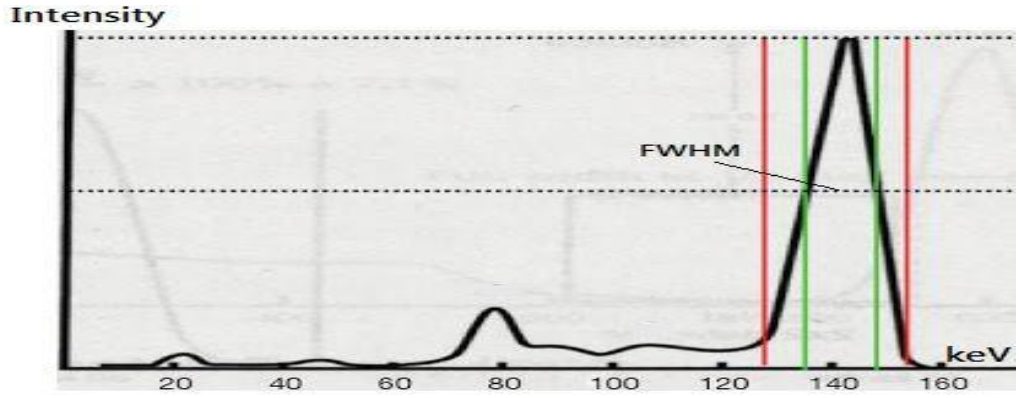

Figure 2.6: Schematic of the full width at half maximum (FWHM) for ^{99m}Tc of 140 keV (Brahme, 2014)

2.5.6 Filtering in SPECT Imaging

Image filtering denotes any operation applied to pixels in an image. In tomographic technique (e.g. SPECT), projections are acquired from many angles around a patient's body by one or more rotating detectors. These data are then reconstructed and assembled to form 3D images of the organ or body. The reconstructed SPECT images of tomographic planes are achieved by two means: filter back projection and iterative projection (Bruyant, 2002). The SPECT image quality is restricted by many factors, such as γ-ray photon scatter and attenuation, detection efficiency and spatial resolution of the collimator–detector system (Tsui, 1996). These effects result in poor spatial resolution, high noise and low contrast; thus, image filtering is highly necessary in SPECT imaging.

Selecting the proper filter and determining its parameters are amongst the obstacles in clinical SPECT reconstruction. Routine image filtering is important, although a filter is mostly subjectively applied in image-processing parameters. In numerous clinical evaluations, literature does not provide useful information for particular imaging filter parameters. In most clinical routine cases, filters are selected experimentally. Moreover, using an appropriate filter type requires a standardised image processing method, which may improve the diagnostic compatibility and interpretation of interdepartmental results.

2.5.7 Filtering by Signal-to-Noise Ratio

Applying a smoothing filter is a popular method to reduce or remove noise from a SPECT image. Such a low-pass filter permits a low frequency to remain unaltered and

avoids high frequencies. Low-pass filters are characterised fundamentally by two parameters, namely, the 'cut-off frequency' and the 'order'. The cut-off frequency is defined as the frequency above which the noise is eliminated. The filter function is zero for all frequencies above the cut-off frequency, which is expressed in cycles per pixel. The cut-off frequency value varies typically from 0.2 to 1.0. These values determine how the filter impacts the resolution and noise. A high value improves the spatial resolution and displays many details in the SPECT image but with much noise. By contrast, a low cut-off frequency value increases the smoothing but degrades the contrast of the SPECT image.

2.5.8 Butterworth Filter

In clinical practice, Butterworth filter is preferred for ^{99m}Tc images (Tsui, 1996). The Butterworth filter is a low-pass filter frequently used in nuclear medicine. It is characterised by two parameters: the critical frequency, which is the point at which the filter begins its roll to zero, and the order. The Butterworth filter can alter not only the critical frequency but also the steepness of the roll-off. Therefore, this filter can simultaneously smoothen and preserve the image resolution. The Butterworth filter can be expressed by the following equation:

$$B(f) = \frac{1}{\left[1+\left(\frac{f}{fc}\right)^{2n}\right]^3} \tag{2.10}$$

where

f is the spatial frequency domain,

f_c is the critical frequency and n is the order of the filter.